Chemical Science

ROYAL SOCIETY OF CHEMISTRY

EDGE ARTICLE

View Article Online
View Journal | View Issue

Cite this: *Chem. Sci.*, 2022, **13**, 218

All publication charges for this article have been paid for by the Royal Society of Chemistry

Received 6th October 2021
Accepted 19th November 2021

DOI: 10.1039/d1sc05484h

rsc.li/chemical-science

HSA-Lys-161 covalent bound fluorescent dye for *in vivo* blood drug dynamic imaging and tumor mapping†

Yongkang Yue,[a] Tingting Zhao,[a] Yuting Wang,[a] Kaiqing Ma,[a] Xingkang Wu,[a] Fangjun Huo,[b] Fangqin Cheng[c] and Caixia Yin *[a]

The specific combination of human serum albumin and fluorescent dye will endow superior performance to a coupled fluorescent platform for *in vivo* fluorescence labeling. In this study, we found that lysine-161 in human serum albumin is a covalent binding site and could spontaneously bind a ketone skeleton quinoxaline–coumarin fluorescent dye with a specific turn-on fluorescence signal for the first time. Supported by the abundant drug binding domains in human serum albumin, drugs such as ibuprofen, warfarin and clopidogrel could interact with the fluorescent dye labeled human serum albumin to feature a substantial enhancement in fluorescence intensity (6.6-fold for ibuprofen, 4.5-fold for warfarin and 5-fold for clopidogrel). The drug concentration dependent fluorescence intensity amplification realized real-time, *in situ* blood drug concentration monitoring in mice, utilizing ibuprofen as a model drug. The non-invasive method avoided continuous blood sample collection, which fundamentally causes suffering and consumption of experimental animals in the study of pharmacokinetics. At the same time, the coupled fluorescent probe can be efficiently enriched in tumors in mice which could map a tumor with a high-contrast red fluorescence signal and could hold great potential in clinical tumor marking and surgical resection.

Introduction

Pharmacokinetics illustrates the dynamic changes, transformations and resulting pharmacological and toxicological significance of drugs and other exogenous substances in the body.[1] As one of the key indicators of pharmacokinetics, blood drug concentration is closely related to its pharmacological effect, which is an important factor for the formulation of dosing regimens and personalized treatment.[2,3] As a generally used methodology, after drugs have been administered to experimental animals, blood concentrations are analyzed through continuous blood sample collection, plasma separation, drug extraction and separation, and mass spectrometry testing.[4,5] For drugs without significant UV-Vis absorption or which are transformed to metabolites in the circulation, the analysis process will be more challenging. In the above processes, multiple blood sampling will not only cause great suffering to the experimental animals, but will also need the consumption of a large number of experimental animals.[6] In addition, the complicated separation and analysis process will inevitably cause detection errors. The development of *in situ* and non-invasive tools for blood drug concentration analysis *in vivo* will fundamentally solve the above dilemma.

Human serum albumin (HSA) is the most abundant protein in plasma. It embodies three alpha helical domains, two Sudlow's sites and cysteine-34 amino acid residue in its structure, so HSA can bind to a variety of exogenous compounds *via* both covalent and non-covalent bonding modes.[7] At the same time, its biodegradable, non-toxic and non-immunogenic properties make it a superior vehicle to achieve drug delivery in the human body, especially for the delivery of hydrophobic drugs.[8–10] Drugs modified by albumin generally prolong the circulation time in the blood, thus showing better pharmacological activity. Combining all these features, nuclear magnetic resonance contrast agent modification or ^{18}F radioactive labeling of HSA as biocompatible blood pool imaging agents could realize the imaging of hemangioma and other circulation diseases *in vivo*.[11]

In our research, we found that 3-acetyl coumarin derivatives could bind to HSA and exhibited significant fluorescence enhancement. We envision that non-covalent binding of drug molecules with fluorescent dye labeled HSA may cause subtle changes in the spatial structure of HSA and therefore affect the

[a]*Key Laboratory of Chemical Biology and Molecular Engineering of Ministry of Education, Shanxi Laboratory for Yellow River, Institute of Molecular Science, Shanxi University, Taiyuan 030006, China. E-mail: yincx@sxu.edu.cn*

[b]*Research Institute of Applied Chemistry, Shanxi University, Taiyuan 030006, China*

[c]*Institute of Resources and Environment Engineering, Shanxi University, Taiyuan, 030006, China*

† Electronic supplementary information (ESI) available: Supplemental experimental procedures, Fig. S1–S16, Tables S1–S4 and compounds characterization figures. See DOI: 10.1039/d1sc05484h

chemical environment of the fluorescent dyes to display different fluorescence signals. Based on the above considerations, we prepared a new coumarin derivative **SS-1** as the fluorescent dye which could bind with HSA to form a coupled fluorescent probe to image the concentration of drugs. **SS-1** responded to HSA with specific turn-on fluorescence responses, and the coexistence of drugs such as ibuprofen, warfarin, clopidogrel *etc.* could amplify the fluorescence intensity significantly (6.6-fold for ibuprofen, 4.5-fold for warfarin and 5-fold for clopidogrel) in aqueous solution. We demonstrated the combination mechanism of HSA with the dye and validated the *in vivo* blood drug concentration monitoring of the coupled fluorescent probe, utilizing ibuprofen as the model drug. The present results present a brand-new methodology to analyze the pharmacokinetics of drugs.

Results and discussion

Fluorescent dye synthesis and optical properties

Coumarin derivatives as fluorescent dyes have long been used for bio-molecule analysis *in vitro* and *in vivo*.[12] In our previous research, we focused on the functionalization of coumarin dyes with versatile applications for small molecule detection with fluorescence responses.[13,14] NMC as a typical coumarin dye was found to interact with HSA in PBS with enhanced fluorescence responses (Fig. S1†). The increasing HSA-induced fluorescence signal blue-shifted from 516 nm to 510 nm, which was caused by the gradually decreasing environmental polarity of the dye.

Compared with the generally used 7-amino coumarin derivatives, the additional introduction of a nitrogen atom as an electron-donating moiety at the 6-position of coumarin could significantly enhance the D–π–A conjugation system to extend the fluorescence emission wavelength.[15] Besides, the alternating vibronic structure was reported to expand the Stokes shift of the dyes efficiently.[16] Thus, we used tetrahydroquinoxalin as a frame to synthesize a coumarin-based fluorescent dye **SS-1** to label HSA with optimized optical properties for bio-imaging. As shown in Fig. 1, the reaction between **SS-1** and HSA induced significant absorbance enhancement at 515 nm. The corresponding fluorescence intensity was enhanced over 16-fold at 595 nm within 5 min in PBS. To evaluate the fluorescence specificity of **SS-1** toward HSA, we then tested the fluorescence responses of **SS-1** upon the addition of various biological molecules, including amino acids, nucleophilic anions, oxidative species, rat serum albumin (RSA), bovine serum albumin (BSA) and HSA. Fig. S2† displays the fluorescence intensities of the tested system. None of them except HSA could induce the turn-on fluorescence response. The specificity was further evaluated upon the addition of human serum to an **SS-1**-containing PBS solution. Upon native-PAGE gel separation (Fig. S3†), the fluorescence-labeled bands were collected, digested and analyzed by LC-MS. Tables S1 and S2† list the corresponding MS results of the two bands highlighted with a red box and a green box, respectively. The narrow band in the green box might reflect more precise protein information. Alpha-1-antitrypsin and HSA were found to be the potential proteins according to the peptide spectrum matched data. In the following SDS-PAGE gel analysis experiments (Fig. S4A and B†), we noticed that **SS-1**-stained human serum displayed a significant fluorescence signal in the range of 55–70 kD in the gel, consistent with the HSA lane. However, the presence of **SS-1** in alpha-1-antitrypsin did not display any fluorescence staining.[17] Fluorescence spectra analysis of **SS-1** and alpha-1-antitrypsin was consistent with the electrophoresis results (Fig. S5†). The abundant potential proteins presented in the MS results were caused by the protein interaction in human serum (Fig. S6†). Thus, **SS-1** modifying HSA in a selective manner can be used for both denatured and nondenatured HSA labeling. The binding molar ratio of **SS-1** and HSA was measured to be 1 : 2 based on the equimolar method (Fig. S7A and B†).[18] The fluorescence intensity of the detection system at 591 nm displayed two-stage linear changes with the concentration of HSA ranging from 0 to 0.4 mg mL^{-1} and from 0.4 to 1 mg mL^{-1}, which could be used for quantifiable HSA analysis. The K_a value of HSA and **SS-1** was calculated to be 5.22×10^4 M^{-1} (Fig. S7D†).

Ibuprofen and warfarin are well-studied small molecule drugs that bind with the hydrophobic binding pockets named Sudlow's site II and Sudlow's site I of HSA, respectively.[8,19] Generally, for HSA-labeled fluorescent dyes based on non-covalent bonding mode, the addition of drugs such as ibuprofen, warfarin and camptothecin would competitively reverse the fluorescence signal changes to some extent.[20,21] In our experiments, we utilized ibuprofen and warfarin initially as the model drugs to test whether their presence could modulate

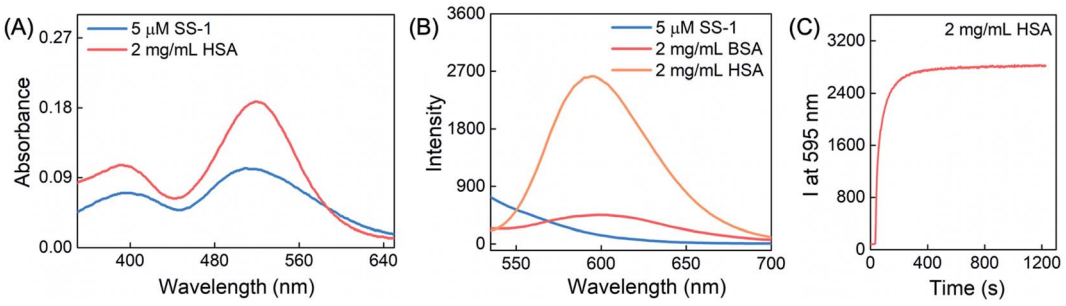

Fig. 1 Optical responses of **SS-1** toward HSA. (A) UV-vis absorption changes upon addition of 2 mg mL^{-1} HSA into a 5 μM **SS-1**-containing PBS system. (B) The corresponding changes in the fluorescence spectra. (C) Time-dependent fluorescence intensity change in the reaction system at 595 nm. λ_{ex} = 505 nm; λ_{em} = 525–700 nm; slit 5/5 nm; 700 V.

the fluorescence responses of **SS-1** toward HSA. Interestingly, instead of the generally found competing fluorescence changes, the addition of ibuprofen or warfarin induced a 6.6-fold or 4.5-fold fluorescence intensity enhancement compared with the HSA–**SS-1** system, respectively (Fig. S8A†). At the same time, ibuprofen-induced fluorescence signal amplification was related to concentration and ibuprofen did not interact with **SS-1** without the presence of HSA in the detection system (Fig. S8B–D and F†). Besides, *in vitro* spectral analysis demonstrated that the complex could quantifiably detect ibuprofen in the hemolyzed rat blood supernatant (Fig. S8G–I†). These results supported our proposal that fluorescent dye labeled HSA could serve as a coupled fluorescent platform for drug analysis. Additionally, commonly used drugs, including clopidogrel (for prevention of blood circulation diseases) and camptothecin (an anticancer drug), were tested using the coupled fluorescent probe in PBS (Fig. S14†). Similar to the fluorescence results for ibuprofen and warfarin, the presence of camptothecin or clopidogrel could also induce a fluorescence enhancement in the detection system.

To support the *in vivo* imaging experiments, we tested the fluorescence response changes of RSA and **SS-1** in the presence of ibuprofen or warfarin in the detection system. Fig. S8E† shows that no significant fluorescence enhancement emerged with or without the presence of ibuprofen or warfarin. These results ensured that the coupled fluorescent probe HSA–**SS-1** was not susceptible to detecting the drugs in mice.

Analysis of binding site between HSA and SS-1

There are three potential covalent modification sites in **SS-1**: (1) the α,β-unsaturated ketone moiety as a typical Michael addition reaction site could react with nucleophilic species such as thiols.[13] (2) The phenolic hydroxyl group in the 2-methoxyphenol moiety might react with the carboxyl compound to form an ester bond under the catalysis of an ester condensation catalyst such as *N*-(3-dimethylaminopropyl)-*N*′-ethyl carbodiimide hydrochloride/1-hydroxybenzotriazole monohydrate.[14] (3) The ketone moiety could reversibly condense with the amino group of amino acids such as lysine to form imines.[22,23] To explore the covalent interaction mode between **SS-1** and HSA and the corresponding fluorescence signal change, the potential covalent modification sites presented above were thoroughly tested.

Cysteine-34 of HSA is a well-used covalent modification site through thiol–maleimide conjugation. We pre-treated HSA with *N*-ethylmaleimide (NEM, a thiol scavenger) and then tested the fluorescence spectra upon addition to the solution of **SS-1**. As shown in Fig. S9A,† NEM did not suppress the fluorescence response of **SS-1** to HSA, which meant that HSA did not react with **SS-1** through the sulfhydryl participating nucleophilic addition reaction process. ^{1}H NMR titration experiments further demonstrated the result (Fig. S10†). Upon addition of HSA to **SS-1** in a mixed solvent of DMSO-d_6/D_2O (2/1, v/v), the proton signals of the quinoxaline–coumarin moiety slightly shifted to the low field while the signals of the 2-methoxyphenol moiety did not display any change. The proton signals of the C=C bond remained exactly the same, which further supported the above conclusions. For the potential covalent binding sites of the phenolic hydroxyl group and ketone moiety, we synthesized two control compounds named **SS-1-E** and **SS-QC-O** (Fig. 2A), which eliminated the two respective sites through chemical modification. The fluorescence spectra responses of the control compounds toward HSA were then tested. Both **SS-1-E** and **SS-QC-O** displayed turn-on fluorescence responses in the presence of HSA in PBS (Fig. 2B). However, after separation by SDS-PAGE gel, except for **SS-QC-O**, both **SS-1** and **SS-1-E** presented HSA bands displaying a significant fluorescence signal (Fig. 2C). Thus, the fluorescence response of **SS-QC-O** toward HSA was caused by non-covalent bonding and the ketone moiety might be the key moiety for HSA labeling by **SS-1**. The result was further verified by a control compound named **SS-QC-ACl** with carbonyl as the reactive site. The dye could label HSA in both aqueous solution and SDS-PAGE gel.

Lysine and arginine are amino acids with a free amino group in proteins, which might react with the ketone to form imines. We then digested the **SS-1**-modified HSA with chymotrypsin and trypsin, respectively, and tested the fragment mass by LC-MS. The results showed that 92.61% coverage was obtained with chymotrypsin and 86.37% coverage with trypsin (Table S3†). The corresponding peptide mass spectra showed that peptide L.KK[+416.174]Y.L, located between 160 and 162 of HSA with the highest score, might be the dominant modified position (Table S4†). Indeed, in the fragment mass spectra, the signals labeled as b1 and y2 matched the calculated mass data exactly (129.1022 for K and 726.3498 for **SS-1**-KY, Fig. S11†). Thus, **SS-1** reacted with lysine-161 of HSA through covalent binding to form the adduct HSA–**SS-1** (Fig. 2). Interestingly, the presence of aspirin in HSA would partly inhibit the fluorescence response after addition to the **SS-1** solution (Fig. S9B†). This result was induced by the esterase activity of HSA in aspirin deacetylation to produce acetylated HSA on the lysine residues which further inhibited the covalent binding of HSA with **SS-1**.[24,25] **SS-1** has no significant fluorescence emission signal in either protic polar solvent (such as PBS or ethanol) or aprotic polar solvent (such as acetonitrile or DMSO). Besides, the increased viscosity did not induce a change in the fluorescence signal of **SS-1** (PBS/glycerol, 1/1, v/v). After condensation with the amino group of lysine-161, the hydrophobic domain would promote the turn-on fluorescence emission (Fig. S9C and D†).

In vitro cellular HSA imaging

The cell imaging capability of **SS-1** was evaluated with HeLa cells. As shown in Fig. 3, HSA-loaded HeLa cells displayed a significant fluorescence signal in the red channel upon further incubation with **SS-1**. Correspondingly, a non-fluorescence signal was observed in the control group. The present result demonstrated that **SS-1** was cell membrane permeable and could image HSA specifically in cells. Besides, compared with rhodamine B, after successive incubation with HSA and **SS-1**, illuminated HeLa cells displayed robust photo-stability upon continuous excitation light irradiation for 2 min (Fig. S12,† 92% quenching for rhodamine B and 40% quenching for HSA–**SS-1**). Thus, the coupled fluorescent probe is more suitable for the long-term fluorescence imaging analysis of biological samples.

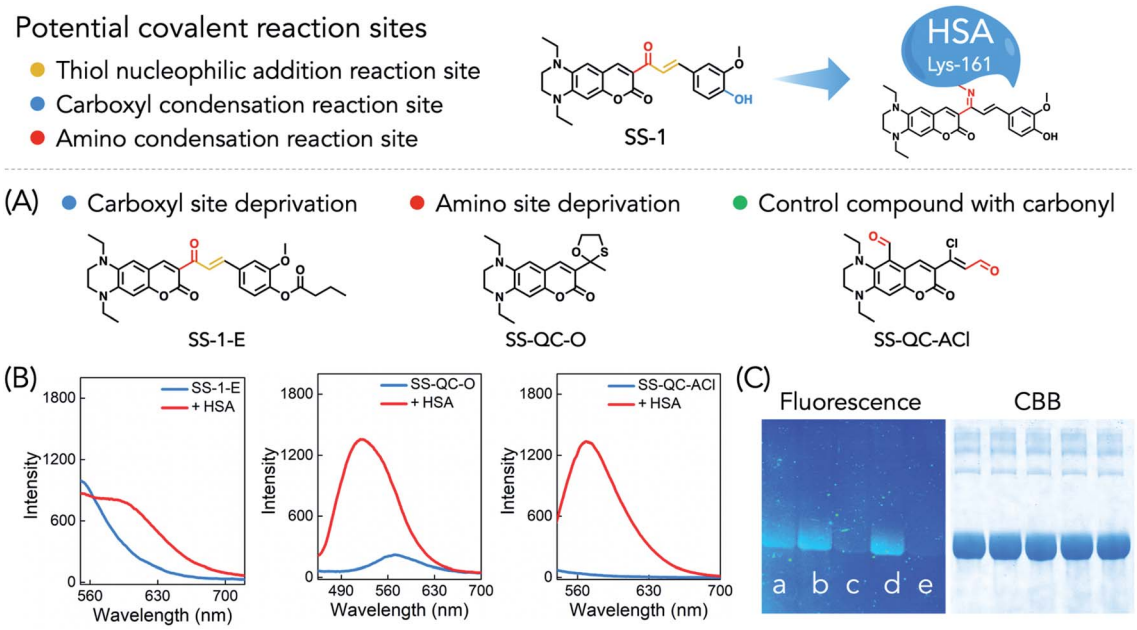

Fig. 2 Covalent binding site verification of HSA and **SS-1**. (A) Reaction site based modification of the fluorescent dyes. (B) Fluorescence responses of 5 μM **SS-1-E**, **SS-QC-O** and **SS-QC-ACl** toward HSA (2 mg mL^{-1} for **SS-1-E**, 0.5 mg mL^{-1} for **SS-QC-O** and **SS-QC-ACl**) in PBS, respectively. **SS-1-E**: λ_{ex} = 516, slit 5/5 nm, 700 V; **SS-QC-O**: λ_{ex} = 440, slit 2.5/5 nm, 700 V; **SS-QC-ACl**: λ_{ex} = 505, slit 2.5/5 nm, 700 V. (C) Covalent labeling verification of HSA by **SS-1**, **SS-1-E**, **SS-QC-O** or **SS-QC-ACl** analyzed by SDS-PAGE gel. (a–d) Represent the addition of the four fluorescent dyes (40 μM) to HSA (1.25 mg mL^{-1}), respectively; (e) is the control group without dye addition.

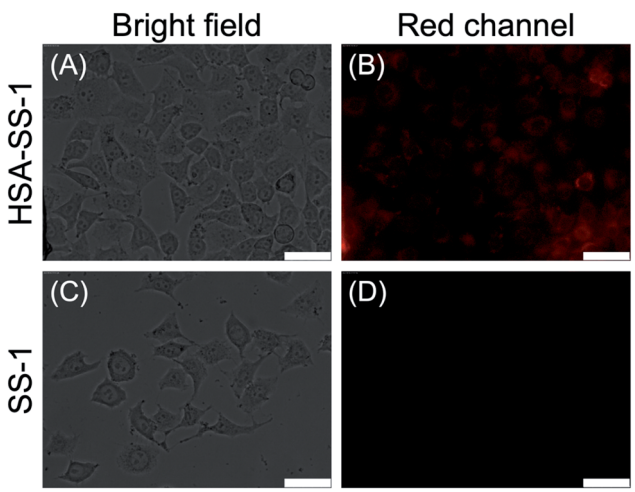

Fig. 3 Fluorescence imaging of HSA in HeLa cells by **SS-1**. (A) Bright field image of HeLa cells incubated with 1 mg mL^{-1} HSA for 1 h and 10 μM **SS-1** for 10 min successively; (B) corresponding fluorescence image of A in the red channel. (C) bright field image of HeLa cells incubated with 10 μM **SS-1** for 10 min; (D) corresponding fluorescence image of C in the red channel. The cells were washed three times with PBS when the medium was changed. λ_{ex} = 536–556 nm; λ_{em} = 560–625 nm. Scale bar = 50 μm.

In vivo ibuprofen monitoring by HSA–SS-1

In order to further verify the feasibility of the coupled fluorescent probe for drug molecule monitoring in the circulation *in vivo*, we first injected HSA–**SS-1** into the blood circulatory system of mice *via* intravenous injection. We noticed that the probe-loaded mice showed a distinct fluorescence signal in the heart area, which was caused by the concentration of blood flow in this area (Fig. 4A). Under the same imaging parameters, mice without probe injection in the control group did not show any fluorescence signal in this area (Fig. 4B). The histogram clearly shows that the increased fluorescence signal in the region of interest (ROI) can indicate the distribution of the coupled fluorescent probe in mice *in vivo* (Fig. 4C).

Supported by the former results, we further set up two sets of mice for the following real-time *in vivo* imaging experiments. Ibuprofen was utilized as the model drug to evaluate the possibility of the coupled fluorescent probe monitoring blood drug concentration changes *in vivo*. Real-time *in vivo* fluorescence imaging of mice administered with HSA–**SS-1** by intravenous injection and ibuprofen suspension by gavage successively displayed periodical fluorescence intensity changes (Fig. 5A and B). Typically, in the first 100 min after administration, the fluorescence intensity of the ROI decreased gradually, which was induced by the physiological metabolism. In the following 120 min, the fluorescence intensity increased and peaked in an overall duration of about 3.5 h after ibuprofen infusion. Further imaging (3.5–5 h) displayed a decrease in the fluorescence intensity. In contrast, the control group without ibuprofen administration showed a constantly decreasing fluorescence intensity change in the ROI (Fig. 5C and D). The *in vivo* fluorescence intensity enhancement was caused by the drug absorption after intragastric administration which gradually concentrated it in the circulation.[26,27]

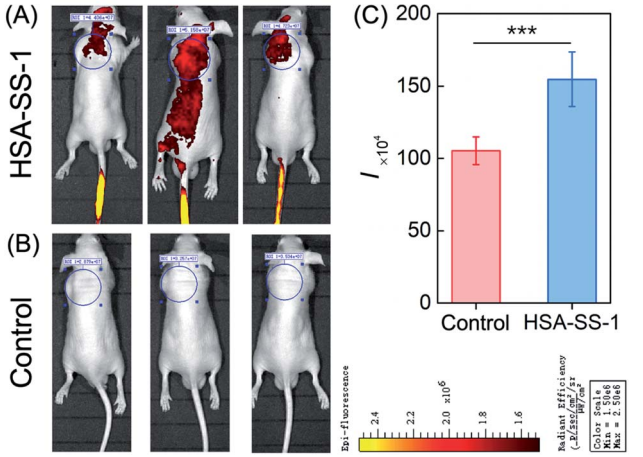

Fig. 4 *In vivo* fluorescence imaging of HSA–**SS-1**. (A) Representative fluorescence images of nude mice captured on an IVIS imaging system 20 min after intravenous injection with 100 μL of PBS solution containing 200 μM HSA, 100 μM **SS-1** and 0.5% DMSO. (B) Mice without injection of the complex as the control group. (C) Histogram of the fluorescence intensities in (A) and (B). Error bars represent standard deviations obtained from five independent experiments. Statistical analyses were performed with Student's *t*-test, ***$p < 0.001$.

The *in vivo* metabolism of HSA–**SS-1** was studied by *ex vivo* organ fluorescence imaging. Mice administered with HSA–**SS-1** by intravenous injection were sacrificed at 20 min and 60 min. Among the vital organs, only the liver displayed a significant fluorescence signal at both of the two time points (Fig. S13†). This meant that the coupled fluorescent probe in the circulation system was mainly metabolized and degraded through the liver.

In vivo cancer targeting by HSA–SS-1

HSA as an efficient drug carrier has widely been used for the delivery of anticancer drugs.[11,28] Its preeminent cancer targeting property is mainly supported by two factors: first, enhanced permeability and retention of tumor tissue induced by leaky defective blood vessels and lack of lymphatic drainage; second, the expression of the albumin-binding proteins, including the gp60 receptor and SPARC in tumor tissue. The has-coupled fluorescent probe was thus used for tumor imaging in nude mice. As shown in Fig. 6A, intravenous injection of HSA–**SS-1** accumulated into the tumor efficiently within 60 min in a spontaneous tumor nude mouse model. The mouse was then sacrificed and the corresponding fluorescence image clearly marked the tumor (Fig. 6B). The dim fluorescence signal in the gut was the spontaneous fluorescence of the mouse feed. Unlike the previously tested distribution of HSA–**SS-1** in the organs of normal mice, the fluorescence signal in the tumor-bearing mouse was only distributed in the tumor and could discriminate the tumor over other organs with high contrast (Fig. 6C). We noticed that the spleen of the nude mouse was significantly enlarged, which is a typical feature of tumor-bearing mice.[29]

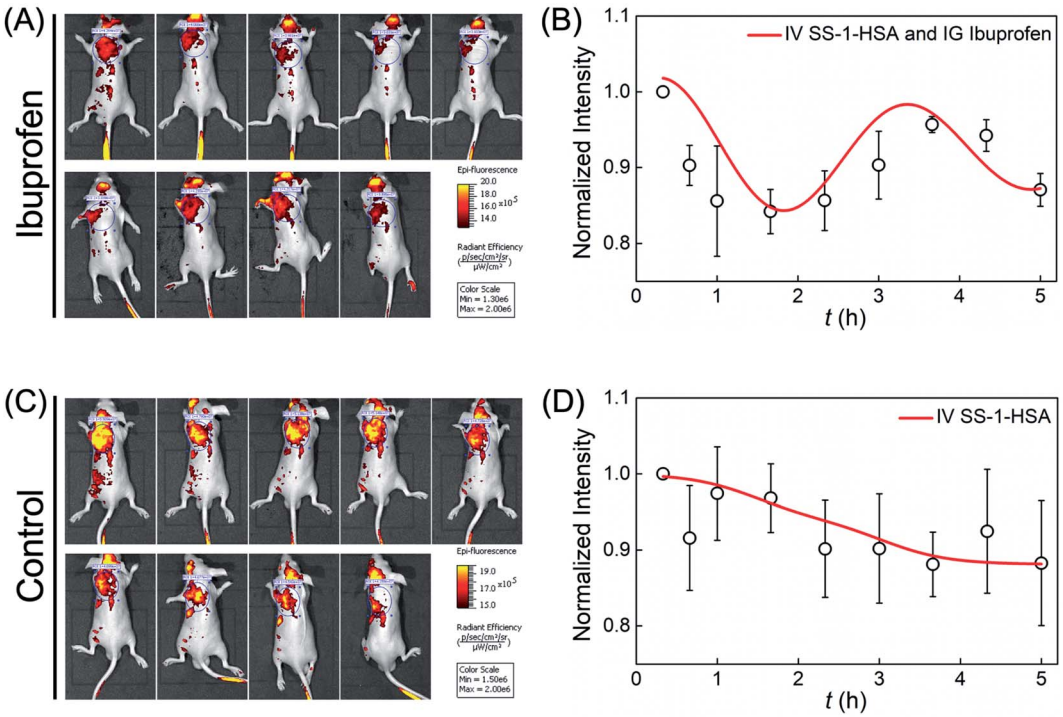

Fig. 5 *In vivo* blood drug concentration monitoring by HSA–**SS-1**. (A) Time-dependent fluorescence images of nude mice captured on an IVIS imaging system. The mice were administered with 100 μL of PBS solution containing 200 μM HSA, 100 μM **SS-1** and 0.5% DMSO *via* intravenous injection and 100 μL of sodium carboxymethyl cellulose suspension containing 2 mg mL^{-1} ibuprofen by gavage. (B) Normalized fluorescence intensities of the ROI in (A). (C) Time-dependent fluorescence images of nude mice administered with 100 μL of PBS solution containing 200 μM HSA, 100 μM **SS-1** and 0.5% DMSO *via* intravenous injection. (D) Normalized fluorescence intensities of the ROI in (C). Error bars represent standard deviations obtained from three independent experiments.

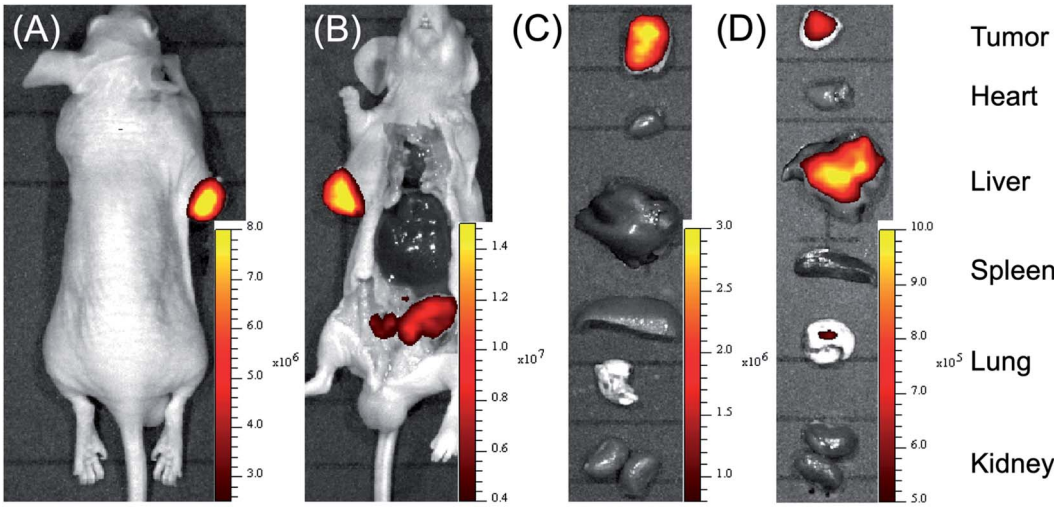

Fig. 6 *In vivo* tumor mapping by HSA–**SS-1**. (A) Fluorescence imaging of spontaneous tumor nude mouse upon intravenous injection of 100 μL of PBS solution containing 200 μM HSA, 100 μM **SS-1** and 0.5% DMSO. The image was taken 60 min after injection. (B) Abdominal imaging of the mouse in (A) after sacrifice. (C) *Ex vivo* organ fluorescence imaging of the mouse in (A). (D) *Ex vivo* organ fluorescence imaging of a xenografted mouse sacrificed 60 min after intravenous injection of 100 μL of PBS solution containing 200 μM HSA, 100 μM **SS-1** and 0.5% DMSO.

Correspondingly, we constructed HeLa cell xenografted mice by subcutaneous injection. After intravenous injection of HSA–**SS-1**, we noticed that the fluorescence signal in the heart area of the mouse decreased gradually, accompanied by enhancement in the subcutaneous tumor (Fig. S15†). *Ex vivo* fluorescence imaging of the vital organs displayed that both the liver and the tumor were stained by the fluorescent probe (Fig. 6D). The fluorescence imaging of the tissue slices obtained from the corresponding organs displayed the same results (Fig. S16†). The partial metabolism of HSA–**SS-1** *via* the liver was mainly due to the slower angiogenesis around the xenograft tumor, which limited the efficient enrichment of HSA–**SS-1** in the tumor.

Based on the above results, we confirmed that HSA–**SS-1** could be used for tumor mapping *in vivo* and could hold great potential in clinical tumor marking and surgical resection.

Conclusions

In conclusion, we reported the specific turn-on fluorescence response of a quinoxaline–coumarin based fluorescent dye named **SS-1** toward HSA *via* the spontaneous covalent binding of lysine-161 and carbonyl with the formation of imines. Compared with rhodamine B, the combination of **SS-1** and HSA exhibited superior photostability, which guaranteed long-term real-time fluorescence detection during *in vivo* imaging. Similar to HSA itself, **SS-1** labeled HSA as a coupled fluorescent probe can also interact with drugs such as ibuprofen, warfarin, clopidogrel and camptothecin. The presence of these drugs induced significant fluorescence intensity enhancement in a drug concentration dependent manner. Thus, based on the coupled fluorescent probe HSA–**SS-1**, we can monitor these invisible drugs by fluorescence signals in real time. The *in vivo* fluorescence imaging results confirmed this proposal. Upon intravenous injection of the fluorescent probe and intragastric administration of ibuprofen, we realized the *in situ* monitoring of blood ibuprofen concentration by fluorescence analysis for the first time. We found that 100 min after intragastric administration, the concentration of ibuprofen in the blood system of mice increased significantly and peaked in an overall duration of about 3.2 h. This result is quite consistent with the blood concentration changes of ibuprofen in humans reported in the literature.[27] Since in this *in situ* analysis model, the has-bound ibuprofen was analyzed directly, we can thus get closer to human trials in a mouse model. Compared with the traditional methodology for blood drug concentration monitoring in a pharmacokinetic study, this non-invasive method can essentially reduce the consumption of experimental animals and alleviate the suffering of animals. In addition, because of the wide drug combination feature of HSA, the *in situ* drug monitoring method has an unbeatable advantage in the analysis of poorly stable drugs such as clopidogrel. Similar to the existing tumor targeting process, HSA–**SS-1** can also be efficiently enriched in tumors to achieve the fluorescent labeling of tumors. The coupled fluorescent probe could map tumors *in vivo* with a high-contrast red fluorescence signal, which holds great potential in clinical tumor marking and surgical resection.

Author contributions

Y. Y. and C. Y. conceived the project. Y. Y., T. Z. and Y. W. synthesized the dyes and conducted photophysical characterization and analysis. Y. Y. and T. Z. performed fluorescence imaging experiments. Y. Y., X. W. and K. M. preformed the gel electrophoresis and proteomic analysis. F. H. characterized structures. All authors participated in writing the manuscript.

Conflicts of interest

There are no conflicts to declare.

Acknowledgements

This study was performed in strict accordance with the Chinese guidelines for the care and use of laboratory animals and was approved by the Institutional Animal Care and Use Committee of Scientific Research in Shanxi University (Taiyuan, China). We thank the National Natural Science Foundation of China (No. 21907062, 22074084, 21878180), Innovative Talents of Higher Education Institutions of Shanxi, Scientific and Technological Innovation Programs of Higher Education Institutions in Shanxi (2019L0031), Shanxi Province "1331 project" key innovation team construction plan cultivation team (2018-CT-1), 2018 Xiangyuan County Solid Waste Comprehensive Utilization Science and Technology Project (2018XYSDJS-05), Shanxi Collaborative Innovation Center of High Value-added Utilization of Coal-related Wastes (2015-10-B3), Key R&D Program of Shanxi Province (201903D421069), the Shanxi Province Science Foundation (No. 201901D111015), Key R&D and transformation plan of Qinghai Province (2020-GX-101), and Scientific Instrument Center of Shanxi University (201512). We are also very grateful for the help of Prof. Hongfei Wang, Prof. Yawei Shi and Prof. Wenming Wang.

References

1 M. Kester, K. D. Karpa and K. E. Vrana, in *Elsevier's Integrated Review Pharmacology*, ed. M. Kester, K. D. Karpa and K. E. B. T.-E. I. R. P., E. Vrana, W. B. Saunders, Philadelphia, 2nd edn, 2012, pp. 1–15.
2 D. J. Reynolds and J. K. Aronson, *Bmj*, 1993, **306**, 48–51.
3 R. Scott Obach, *Pharmacol. Rev.*, 2013, **65**, 578–640.
4 A. Veringa, M. G. G. Sturkenboom, B. G. J. Dekkers, R. A. Koster, J. A. Roberts, C. A. Peloquin, D. J. Touw and J. W. C. Alffenaar, *TrAC, Trends Anal. Chem.*, 2016, **84**, 34–40.
5 A. Telekes, M. Hegedűs and I. Kiss, in *Medical Applications of Mass Spectrometry*, ed. K. Vékey, A. Telekes and A. B. T.-M. A. of M. S. Vertes, Elsevier, Amsterdam, 2008, pp. 263–289.
6 D. Zhang, C. E. C. A. Hop, G. Patilea-vrana, G. Gampa, H. K. Seneviratne, J. D. Unadkat, J. R. Kenny, K. Nagapudi, L. Di, L. Zhou, M. Zak, M. R. Wright, N. N. Bumpus, R. Zang, X. Liu, Y. Lai, S. C. Khojasteh, S. S. Francisco and D. Z. California, *Drug Metab. Dispos.*, 2019, **47**, 1122–1135.
7 E. N. Hoogenboezem and C. L. Duvall, *Adv. Drug Delivery Rev.*, 2018, **130**, 73–89.
8 G. Rabbani and S. N. Ahn, *Int. J. Biol. Macromol.*, 2019, **123**, 979–990.
9 G. Yang, S. Z. F. Phua, W. Q. Lim, R. Zhang, L. Feng, G. Liu, H. Wu, A. K. Bindra, D. Jana, Z. Liu and Y. Zhao, *Adv. Mater.*, 2019, **31**, 1–9.
10 Z. Liu and X. Chen, *Chem. Soc. Rev.*, 2016, **45**, 1432–1456.
11 G. Fanali, A. Di Masi, V. Trezza, M. Marino, M. Fasano and P. Ascenzi, *Mol. Aspects Med.*, 2012, **33**, 209–290.
12 D. Cao, Z. Liu, P. Verwilst, S. Koo, P. Jangjili, J. S. Kim and W. Lin, *Chem. Rev.*, 2019, **119**, 10403–10519.
13 Y. Yue, F. Huo, F. Cheng, X. Zhu, T. Mafireyi, R. M. Strongin and C. Yin, *Chem. Soc. Rev.*, 2019, **48**, 4155–4177.
14 Y. Yue, F. Huo and C. Yin, *Chem. Sci.*, 2021, **12**, 1220–1226.
15 A. R. Jagtap, V. S. Satam, R. N. Rajule and V. R. Kanetkar, *Dyes Pigm.*, 2009, **82**, 84–89.
16 T. B. Ren, W. Xu, W. Zhang, X. X. Zhang, Z. Y. Wang, Z. Xiang, L. Yuan and X. B. Zhang, *J. Am. Chem. Soc.*, 2018, **140**, 7716–7722.
17 H. Iwashita, E. Castillo, M. S. Messina, R. A. Swanson and C. J. Chang, *Proc. Natl. Acad. Sci. U. S. A.*, 2021, **118**, 1–9.
18 Z. Luo, T. Lv, K. Zhu, Y. Li, L. Wang, J. J. Gooding, G. Liu and B. Liu, *Angew. Chem., Int. Ed.*, 2020, **59**, 3131–3136.
19 Y. Huang, T. Lv, T. Qin, Z. Xu, L. Wang and B. Liu, *Chem. Commun.*, 2020, **56**, 11094–11097.
20 G. Chakraborty, A. K. Ray, P. K. Singh and H. Pal, *Chem. Commun.*, 2018, **54**, 8383–8386.
21 K. Zhu, T. Lv, T. Qin, Y. Huang, L. Wang and B. Liu, *Chem. Commun.*, 2019, **55**, 13983–13986.
22 L. Pu, *Angew. Chem., Int. Ed.*, 2020, **59**, 21814–21828.
23 E. K. Feuster and T. E. Glas, *J. Am. Chem. Soc.*, 2003, **125**, 16174–16175.
24 M. S. Liyasova, L. M. Schopfer and O. Lockridge, *Biochem. Pharmacol.*, 2010, **79**, 784–791.
25 H. Watanabe, S. Tanase, K. Nakajou, T. Maruyama, U. Kragh-Hansen and M. Otagiri, *Biochem. J.*, 2000, **349**, 813–819.
26 N. M. Davies, *Clin. Pharmacokinet.*, 1998, **34**, 101–154.
27 K. S. Albert and C. M. Gernaat, *Am. J. Med.*, 1984, **77**, 40–46.
28 F. Kratz, *J. Controlled Release*, 2014, **190**, 331–336.
29 M. F. Woodruff and M. O. Symes, *Br. J. Cancer*, 1962, **16**, 120–130.